http://ansinet.com/itj

ITJ

ISSN 1812-5638

INFORMATION TECHNOLOGY JOURNAL

ANSInet
Asian Network for Scientific Information
308 Lasani Town, Sargodha Road, Faisalabad - Pakistan

Information Technology Journal 6 (7): 1057-1062, 2007
ISSN 1812-5638

Endothelial Cell Image Enhancement Using Non-Subsampled Image Pyramid

[1]Mohammad A.U. Khan, [2]M. Khalid Khan, [3]M. Aurangzeb Khan and [4]M. Talal Ibrahim
[1]Department of Electrical Engineering,
COMSATS Institute of Information Technology, Abbottabad, Pakistan
[2]Centre for Image Analysis, Uppsala University, Uppsala, Sweden
[3]Department of Electrical Engineering, COMSATS Institute of Information Technology, Islamabad, Pakistan
[4]Department of Computer Engineering, Center for Advanced Studies in Engineering, Islamabad, Pakistan

Abstract: A corneal endothelial cell image provides vast amount of information about a human eye. The cell density and cell shape parameters of a given endothelial cell image help ophthalmologists in making many vital clinical decisions. The acquired endothelial image is poor in contrast where cell boundaries are masked in the background. Previously, most of the work was based on morphological operations in spatial domain. However, if we think of cell structure as texture hidden in noisy background, we can get help from wavelet-texture segmentation, a well studied area. In this study, we propose a non-subsampled Wavelet pyramid decomposition of lowpass region. At certain level of the pyramid, we start observing cleaner cell boundary structure which greatly facilitates its segmentation. Once segmented automatic cell counting can be used and simulation results have shown improvement in cell density count.

Key words: Endothelial cell images, image pyramids, wavelets, image enhancement

INTRODUCTION

A vast amount of information about the human eye can be gathered through a corneal endothelium. The corneal endothelium is a single hexagonal cell layer. An infant's endothelial cell count begins at 3500 to 4000 cells mm^{-2}. As individuals grow, the cell count declines; adults typically only have 1500 to 2000 cells mm^{-2} of endothelium. The endothelium's chief function is to remove fluid from the corneal stroma, allowing the cornea to remain optically clear. Certain diseases that damage the corneal endothelium, such as Fuchs corneal dystrophy, lead to endothelial changes such as guttae and eventually lead to corneal edema. These individuals often require a corneal transplantation since endothelial cells do not regenerate significantly when damaged. Additional factors that can damage the corneal endothelium usually come from trauma; often, a long cataract case, especially when extracting a large mature cataract, may lead to endothelial damage and cell loss. Sometimes, patients with relatively few endothelial cell counts undergoing cataract surgery may require extended periods to resolve their corneal edema, chiefly because only a few endothelial cells are pumping fluid out of the stroma and into the anterior chamber. Younger patients are relatively much more likely to recover after traumatic insult to the endothelium because they tend to have many more endothelial cells compared with elderly individuals.

Specular microscopes have long been useful instruments to visualize the corneal endothelium. All the information like cell count, cell area, cell density and cell hexagonality is gathered by analyzing the endothelial cell image. To properly analyze cell images it is required that cell boundaries be extracted from its background. From signal processing point of view this extraction lands in the area of image segmentation. In general, endothelial cell images acquired have low contrast, non-homogeneous background intensities across the image due to non-uniform illumination, irregular shapes and thermal noise introduced by acquisition devices. Due to these problems, segmentation and subsequent analysis becomes hard if not impossible. Example of a typical cell image is shown in Fig. 1.

For the segmentation of endothelial cell images several techniques have been investigated in the past such as histogram based and minimum-error-threshold (Ridler and Calverd, 1978) and an active contour-based method for segmentation of white blood cells is proposed by Theeraapattanakul *et al.* (2004) in which a snake like

Corresponding Author: Muhammad A.U. Khan, Department of Electrical Engineering,
COMSATS Institute of Information Technology, University Road, Post Code 22060, Abbottabad,
Pakistan Tel: ++92 992 111 001 007, ++ 333 5264373 Fax: ++92-0992-383441

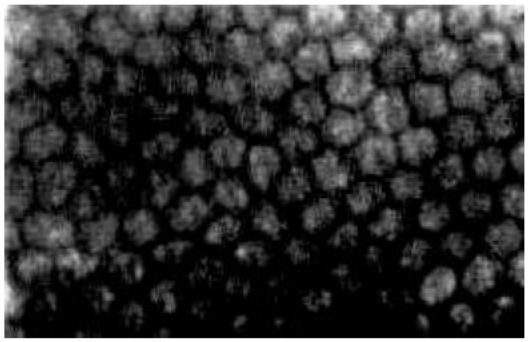

Fig. 1: Original endothelial cell image of size 165×289. Image is low in contrast, non-uniformly illuminated and contains thermal noise

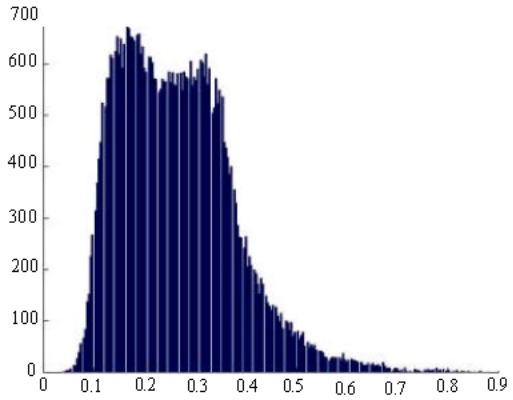

Fig. 2: Histogram of endothelial cell image shown in Fig. 1

shape is allowed to grow to fit the shape of individual blood cell. Caetano *et al.* (2000) proposed a segmentation method based on morphological reconstruction filters, where in an adaptive contrast enhancement and segmentation method is used (Nadachi and Nunokawa, 1992). The segmentation approaches discussed above make use of spatial domain filtering, which will result in the deformation of cell boundaries to some extent. This will further necessitate the use of manual editing of cell boundaries at the end. However, if one sees the cell boundary structure as a texture hidden in a noisy background, we may get help from the rich texture segmentation literature (Song *et al*., 2003; Peng *et al*., 2004). Texture segmentation has been successfully implemented using Wavelet transform.

In present proposed scheme after preprocessing the image, we apply Wavelet transform in a pyramid structure. By observing various output images at different levels of pyramids, we select the one that contains complete cell boundary structure with uniform background.

CHARACTERISTICS OF CELL IMAGE

A typical cell image is shown in Fig. 1. Following are the notable characteristics of this image and many others that we have encountered.

- The contrast between the cell boundaries and background is low. This fact is indicated by the shown histogram of cell image in Fig. 2. The histogram is a uni-modal: one peak. The peak in the histogram corresponds to the intensity of the background pixels, since those pixels are greater in number in cell images.
- Background intensities across the image are not homogeneous due to uneven illumination. This causes cells in one portion of the image to be lighter than cells in another portion.
- Intensities of pixels within a cell vary widely. Intensity variation within a cell causes part of the cell to be labeled as background pixels. This also results in false boundaries.
- Cell shapes are irregular.

Furthermore, some cells are grouped together to form cell clusters. It is evident that cell images of this type possess poor characteristics that make cell segmentation a difficult task. Furthermore, the segmentation problem is even worse when artifacts such as membrane blebbing and cellular fragments exist in the images.

THE PROPOSED SYSTEM

The block diagram of proposed system is shown in Fig. 3. Each process shown is explained in later subsections. The outputs of Frangi's method block are manually examined the match between our output image cell boundaries and the original cell structure. The best overall match is selected for post-processing.

Preprocessing: After acquiring corneal endothelial cell images, we need to pre-process the image for a smooth look. This step involves removal of gray-scale gradient and noise. For the removal of non-uniform illumination, which is in the form of a gradient we have used a lowpass filter of radius $\pi/16$ to get the illumination pattern and then subtracted it from the original cell image. An adaptive median filter that eliminates thermal noise in the

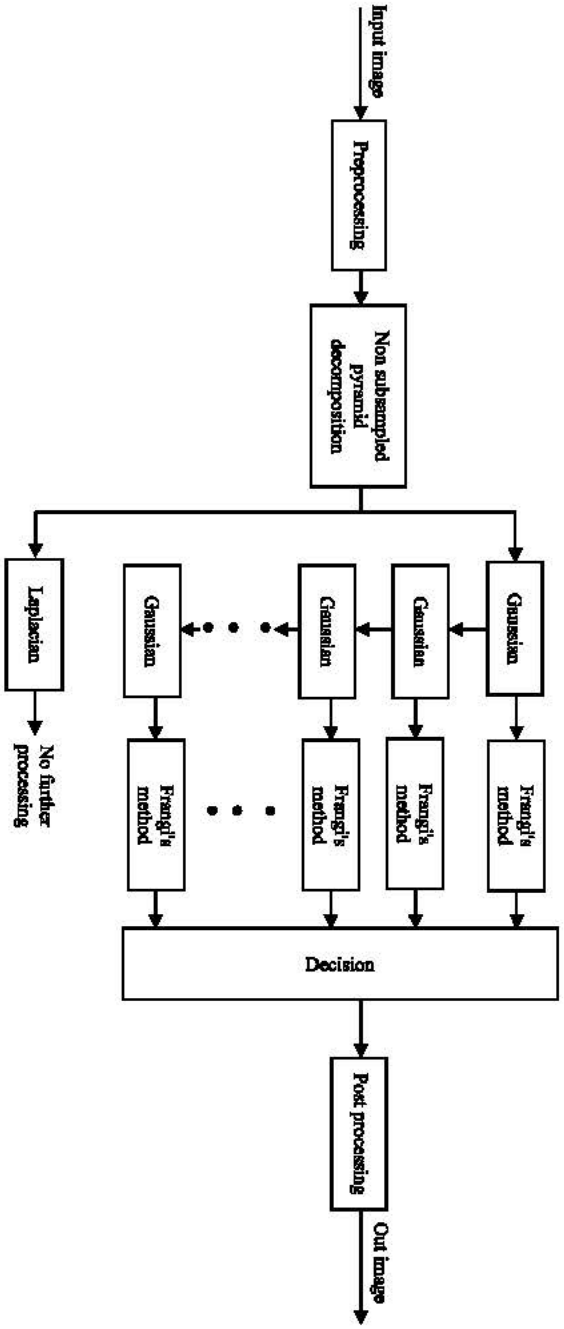

Fig. 3: Block diagram of proposed system

image is applied. Loss of detailed information due to this filtering is negligible as the cell boundary width is wider than the filter length and further median filtering avoids edge degradation (Gonzalez and Woods, 2002). Resultant image after preprocessing steps is shown in Fig. 4.

Wavelet non-subsampled pyramid structure: Wavelet transform has gained its popularity as it was successfully

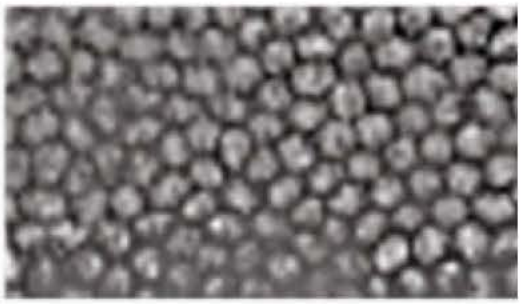

Fig. 4: Image after correction of non-uniform illumination and thermal noise elimination

employed in image compression (Martin and Bell, 2001), image enhancement (Hatami *et al*., 2005), image denoising (Zhong and Ning, 2005), texture segmentation (Sun *et al*., 2004) and image retrieval (Liapis and Tziritas, 2004). Wavelets are orthogonal basis functions, having compact support in time (space), which can be used to represent a signal (image). Unlike conventional Fourier transform, which utilizes sines and cosines of varying amplitude and frequency as its basis functions, wavelet transform makes use of these wavelet functions which are scalable. A variety of such functions exists and a well suitable wavelet can be selected particular to an application depending on the signal/image characteristics to represent.

One of the most striking and powerful applications of wavelet theory is the possibility of multiresolution analysis, shown by Mallat (1987). Multiresolution analysis allows us to exploit the signal or image characteristics, matched to a particular scale, which might go undetected in other analysis techniques. This capability of multiresolution processing paved the way to successful analysis of various kinds of texture. Large image such as remote sensing image always comprise a good many texture information. Texture can be defined as an attribute representing the spatial arrangement of the gray levels of the pixels in a region. The sole aim of a texture analysis method is to describe different textures present in an image.

The most important aspects of texture description have been identified at different scales. If we can collect these descriptive features corresponding to a texture at various scales, we can distinguish different textures in an image. As cell boundary in endothelial images can be thought of as coarse texture and this texture can easily be modeled through low frequency signals (Pemmaraju *et al*., 1995). Due to this very reason we concentrate on low frequency region of endothelial cell image. We start

constructing image pyramid by decomposing given cell image into its Gaussian and Laplacian pyramid as discussed in (Adleson *et al*., 1984). The low frequency nature of the texture forces us to build Gaussian pyramid only. The bottom or zero level of Gaussian pyramid G_0 is equal to the original image. It is lowpass filtered to obtain next pyramidal level G_1. G_1 is filtered in the recursive fashion to obtain finer levels.

In this research, we have used non-subsampled pyramidal decomposition where downsamplers have been removed to provide correspondence between two pixels located at the same spatial index (n_1, n_2) in two different levels. As it is a non-subsampled decomposition so output images once stacked will not form pyramid rather a tower with equal-size floors. The cell image corresponding to seventh level of non-subsampled Gaussian pyramid is shown in Fig. 5. Comparing Fig. 5 with Fig. 4, we see that cell boundaries are much cleaner.

Cell boundaries enhancement: Image shown in Fig. 5 have smooth look and better in contrast but still lack continuity due to varying contrast among cell boundaries. In order to provide continuous map of cell boundaries we are in need of tracking algorithms. One popular vessel tracking algorithm for angiogram images is described in (Frangi *et al*., 1998) and is commonly referred to as Frangi's method. Frangi's method is originally proposed for detection of elongated-tubular-shaped vessel structures which exist with varying contrast. The approach applies second order differentials and vesselness measure to continuously track the complete vessel structure. Images from various levels of Gaussian pyramid are providing a vessel like structure where the cell boundaries can be substituted for vessels. Frangi's method of vessel enhancement has been applied with appropriate parameters to the output of various levels of the Gaussian pyramid. The resulting images are shown in Fig. 6. It is obvious from the images shown in Fig. 6 that as we move up the levels we get cleaner boundary structure. By manual examination of boundary structure we select an appropriate level of decomposition. In case of endothelial cell image shown in Fig. 1, seventh level of Gaussian pyramid is selected to be optimal.

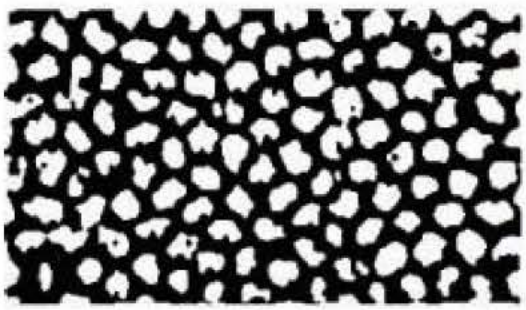

Fig. 5: Image after wavelet pyramidal decomposition

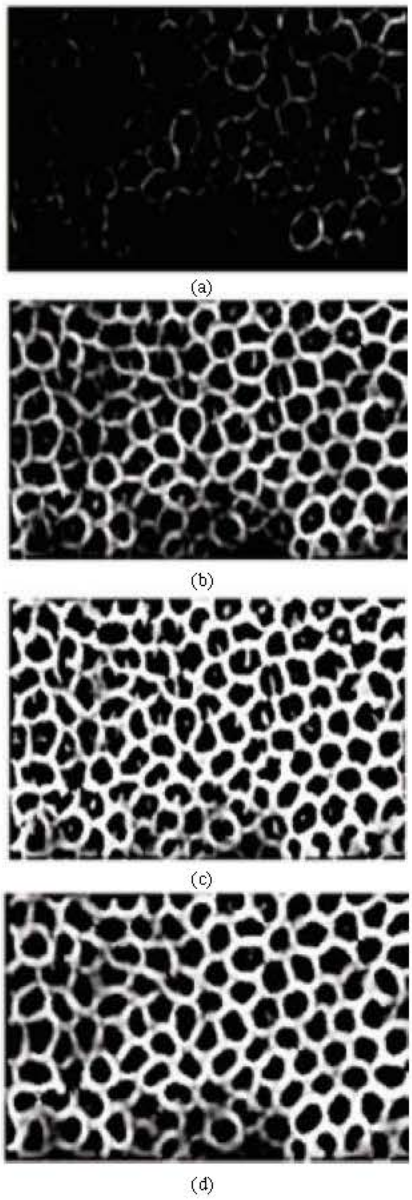

Fig. 6: Resulted images after detection of cell boundaries. Frangi's method is applied on (a) output image of second level of Gaussian pyramid i.e., G_1, (b) output image of third level G_2, (c) output of fourth level G_3 and (d) seventh level of Gaussian pyramid G_6. We see that as we move up the levels, we start getting complete cell boundary structure

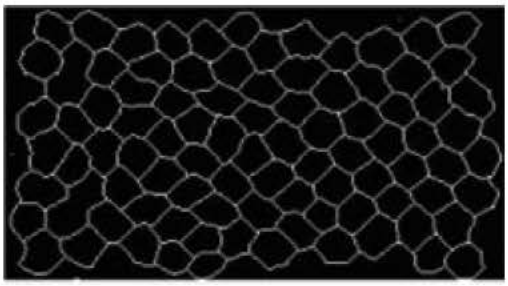

Fig. 7: Final binarized image

Fig. 8: Final result of boundary detection

Post-processing: After selecting the optimal output cell image of Frangi's method, next task is to binaries it. For this purpose morphological operators come handy. The common morphological operators involved in our post-processing include dilation, erosion, opening and closing. First we dilate the image which gradually enlarges the cell boundaries so the holes within the boundaries get filled. After dilation, thinning process is performed to make the boundaries one-pixel wide and at the end, pixels with one or no neighbor, are removed to get rid of false boundaries. Image after all these morphological operations is shown in Fig. 7. Figure 8 shows binarised image superimposed on original image. The binarised image is fed to an automatic counting system (Chen *et al*., 1999). In this counting process cells centers are located and they are labeled and segmented. Now the image contains white dots with black background. The white dots are counted which provides cell density.

RESULTS AND DISCUSSION

The results of our proposed method are better than the results with other automated methods we have experienced. The effect of the pyramidal decomposition and Frangi's method can be seen easily, especially in low-contrast and non-uniformly illuminated images most boundaries are detected correctly.

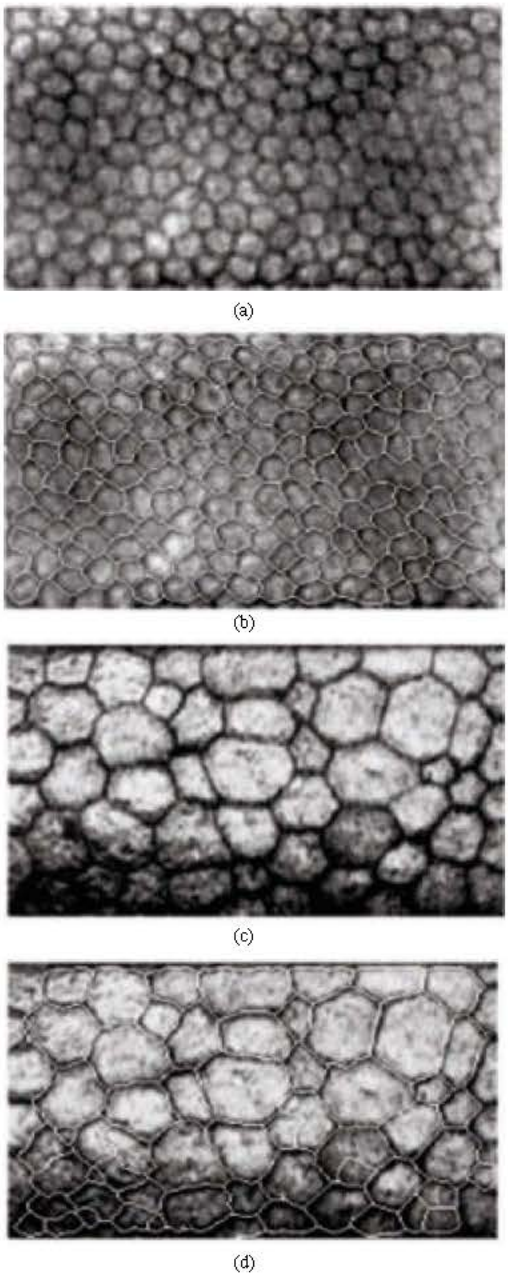

Fig. 9: a) and c) are the two original endothelial cell images whereas b) and d) are final output images of proposed system

We compared the results of our proposed process with the traditional method using three different images. Figure 9 shows two original endothelial cell images and their corresponding output images obtained by proposed

Table 1: Comparison of proposed system and traditional system

	Proposed system			Traditional system		
No.	Cells density	Mean	SD	Cells density	Mean	SD
1	3197.5	299.7	71.1	3140.0	321.7	85.9
2	1949.9	532.0	131.4	1872.3	550.2	170.5
3	2052.7	446.1	152.3	1974.3	449.3	156.9

system. Table 1 gives comparison of two methods in terms of cell density, mean cell size and Standard Deviation (SD). The difference in the mean cell size between the two methods is less than 5%. Differences in cell size standard deviation are slightly larger. The mean cell size is calculated from the total area of the analyzed region and the number of cells in the region. Therefore, the results of the two methods may be comparable if the same number of cells is determined, regardless of the individual sizes.

Even though some future improvements are necessary, proposed method provides accurate analysis of the endothelial cell image, which will be welcomed in clinical practice.

REFERENCES

Adleson, E.H., C.H. Anderson, J.R. Bergen, P.J. Burt and J.M. Ogden, 1984. Pyramid methods in image processing. RCA Eng., 29: 33-41.

Caetano, C.A.C., L. Ventura, S.J.F. Sousa and R.D.A. Lotufo, 2000. Identification and segmentation of cells in images of donated corneas using mathematical morphology. In: Proceedings of XII Brazillian Symposium on Computer Graphics and Image Processing, Oct. 2000.

Chen, Y., K. Biddell, A. Sun, P.A. Relue and J.D. Johnson, 1999. An automatic cell counting method for optical images. In: Proceedings of 1st Joint BMES/EMBS Conference Serving Humanity Advancing Technology, Oct. 1999.

Frangi, A., W.J. Niessen, K.L. Vincken and M.A. Viergever, 1998. Multiscale vessel enhancement filtering. In: 1st International Conference of Medical Image Computing and Computer Assisted Intervention (MICCAI, 1998).

Gonzalez, R.C. and R.E. Woods, 2002. Digital Image Processing. Pearson Education, Prentice Hall.

Hatami, S., R. Hosseini, M. Kamarei and H. Ahmadi, 2005. Wavelet based fingerprint image enhancement. In: Proceedings of IEEE International Symposium on Circuits and Systems. May 2005.

Liapis, S. and G. Tziritas, 2004. Color and texture image retrieval using chromaticity histograms and wavelet frames. IEEE Trans. Multimedia, 6: 676-686.

Mallat, S., 1987. A compact multiresolution representation: The wavelet model. In: Proceedings of IEEE Computer Society Workshop on Computer Vision. Washington, DC.

Martin, M.B. and A.E. Bell, 2001. New image compression techniques using multi-wavelets and multi-wavelet packets. IEEE. Trans. Image Processing, 10: 500-510.

Nadachi, R. and K. Nunokawa, 1992. Automated corneal endothelial cell analysis. In: Proceedings of 5th Annual IEEE Symposium on Computer-Based Medical Systems, June 1992.

Pemmaraju, S., S. Mitra, Y.Y. Shieh and G.H. Roberson, 1995. Multiresolution wavelet decomposition and neuro-fuzzy clustering for segmentation of radiographic images. In: proceedings of 8th IEEE International Symposium on Computer-Based Medical Systems, June 1995.

Peng, L., Z.M. Zhao and J.L. Ma, 2004. Texture image segmentation based on wavelet-domain hidden markov models. In: Proceedings of IEEE International Geosciences and Remote Sensing Symposium.

Ridler, T. and S. Calvard, 1978. Picture thresholding using an iterative selection method. IEEE. Trans. Syst. Man Cybernetics, 8: 630-632.

Song, X.F., Z.G. Chen, C.L. Wen and Q.B. Ge, 2003. Wavelet transform-based texture segmentation using feature smoothing. In: Proceedings of International Conference on Machine Learning and Cybernetics, Nov. 2003.

Sun, J., D. Gu, S. Zhang and Y. Chen, 2004. Hidden markov Bayesian texture segmentation using complex wavelet transform. In: IEE Proceedings on Vision, Image and Signal Processing, June 2004.

Theeraapattanakul, J., J. Plodpai and C. Pintavirooj, 2004. An efficient method for segmentation step of automated white blood cell classification. In: Proceedings of IEEE Region 10 Conference on TENCON, Nov. 2004.

Zhong, J. and R. Ning, 2005. Image denoising based on wavelets and multi-fractals for singularity detection. IEEE Trans. Image Processing, 14: 1435-1447.